ELSEVIER

Journal of Alloys and Compounds 408–412 (2006) 675–679

Journal of ALLOYS AND COMPOUNDS

www.elsevier.com/locate/jallcom

Optical properties and local structure of rare-earth-doped amplifier for broadband telecommunication

Setsuhisa Tanabe *

Graduate School of Human and Environmental Studies, Kyoto University, Sakyo-ku, Kyoto 606-8501, Japan

Received 30 July 2004; received in revised form 17 December 2004; accepted 13 January 2005
Available online 14 July 2005

Abstract

Optical properties and local structure of rare-earth ions in glasses for broadband optical fiber amplifiers are reviewed. In a series of Er-doped glasses with broad 1.5 μm emission, heavy-metal oxide glasses are attracting great interest. Anomalous compositional dependences of optical properties of Er-doped antimony silicate glasses are shown. Structural implication of small compositional dependence observed for the Judd–Ofelt Ω_6 parameter and local phonon energy are discussed.

Keywords: Amorphous materials; Luminescence

1. Introduction

Due to rapid increase of information traffic and the need for flexible networks, there exists urgent demand for optical amplifiers with a wide and flat gain spectrum in the telecommunication window, to be used in the wavelength-division-multiplexing (WDM) network system. After the invention of the Er-doped fiber amplifier (EDFA), various types of amplifier devices have been developed in order to broaden the telecommunication bandwidth in the WDM network [1]. Tm^{3+}-doped and Pr^{3+}-doped fluoride fiber amplifiers have been developed for the S-band and O-band applications, respectively. Long-term reliability of fluoride fibers is still an issue for practical use [2]. The Raman amplifier composed of conventional silica fiber is also becoming practical use in WDM system that requires small gain (∼10 dB) in broad wavelength range. The gain range and bandwidth can be controlled by the wavelength and configuration of pumps. However, the pump power required is very high compared with the rare-earth-doped fiber amplifiers. Still the rare-earth-doped amplifiers can be promising in the practical system due to their high power conversion efficiency.

Most of the EDFA utilized at present is made of silica-based glass fiber, where doped Er^{3+} ions show narrow emission band at 1.55 μm resulting in narrow gain spectra. Following the report of wide spectra [3], Mori et al. reported excellent performance of a tellurite-based EDFA [4], which shows 80 nm wide gain around 1.53–1.61 μm. In order to increase the channels and to improve the performance of WDM network, it is important to investigate a material with wider gain spectra. We have reported that the Bi_2O_3-based borosilicate glass showed broad emission spectra of the 1.55 μm transition and large Ω_6 of Er^{3+} ion [5]. In 2001, a group of Corning reported the multi-component silicate (MCS) glass containing Sb_2O_3, which shows wider gain than the glasses [6]. The important factor dominating the cross-section and its bandwidth is the Judd–Ofelt Ω_6 parameter of Er^{3+} ions [7] as well as the refractive index. We also reported a strong correlation between the Ω_6 and the ionicity of Er-ligand bond in various glasses and its origin [8,9]. Therefore, it is interesting to investigate glass systems giving ionic ligand fields, which would attain a large Ω_6.

We report the optical properties of the oxide glass compositions based on Sb_2O_3 in which Er^{3+} ions show very broad emission and the local structure of rare-earth ion in this glass.

* Tel.: +81 75 753 6832; fax: +81 75 753 6634.
E-mail address: stanabe@gls.mbox.media.kyoto-u.ac.jp.

0925-8388/$ – see front matter © 2005 Elsevier B.V. All rights reserved.
doi:10.1016/j.jallcom.2005.01.106

2. Experimental

Glasses in the composition of $x$$Sb_2O_3$–$3Al_2O_3$–$(97-x)SiO_2$ ($x=27$, 37, 47, 57 and 67) doped with 0.5 mol% Er_2O_3 and those doped with 0.5 mol% Eu_2O_3 were prepared by melting mixed powders in an alumina crucible at 1100–1450 °C. The obtained glasses were cut into 15 mm × 10 mm × 3 mm shape before polishing into optical surface.

Emission spectra were measured by using a 970 nm laser diode (LD) and an InGaAs photodiode (160 kHz). The lifetime of the 1.53 μm emission was measured by pumping with light pulses of the LD and the time evolution of the signal of the detector was collected with a 100 MHz digital oscilloscope. Decay curves were analyzed by a least-square fitting to get the lifetime.

The number of Er^{3+} ions in unit volume, ρ_N, was calculated with the molecular weight and density. Density of the obtained glass was measured by the Archimedes method using kerosene as an immersion liquid. The refractive index, $n(\lambda)$, was measured by a prism coupling method at wavelength of 633 nm, 1304 nm and 1550 nm. Absorption spectra were measured in 400–1700 nm with Shimadzu UV-3101PC spectrophotometer. With an integrated area of the absorption band, spontaneous emission probability, A, of the 1.5 μm was calculated by [5],

$$A(J \rightarrow J') = \frac{(2J+1)8\pi cn^2}{(2J'+1)\bar{\lambda}^4} \int_{1.4\mu m}^{1.7\mu m} \frac{k(\lambda)}{\rho_N} d\lambda \quad (1)$$

where c is the light velocity, $\bar{\lambda}$ the mean wavelength of emission, J and J' the total momentum for the upper and lower levels, $k(\lambda)$ the absorption coefficient and n is the refractive index at wavelength of 1530 nm.

The Judd–Ofelt parameters of Er^{3+} ions were calculated by the method described elsewhere [8] with cross-sections of five intense bands ($^4F_{7/2}$, $^2H_{11/2}+{}^4S_{3/2}$, $^4F_{9/2}$, $^4I_{11/2}$ and $^4I_{13/2}$) in 470–1700 nm.

The excitation spectra of the $^5D_0 \rightarrow {}^7F_2$ emission at 613 nm of Eu^{3+}-doped glasses was measured in the range of 440–470 nm with a Shimadzu R500 Fluorescence Spectrophotometer. The phonon sideband associated with the pure electronic $^5D_2 \leftarrow {}^7F_0$ transition 465 nm was multiplied by 50 times to investigate the phonon mode coupled to rare-earth ions [10], which contributes to multi-phonon relaxation.

3. Results and discussion

3.1. Properties of glass and spectroscopy of rare-earth ions

Fig. 1 shows that the compositional dependence of refractive index, $n(\lambda)$, of the glasses at 633 nm and 1550 nm increased with decreasing wavelength. The n of the $x$$Sb_2O_3$–$3Al_2O_3$–$(97-x)SiO_2$ glasses (in mol%) at 1.55 μm

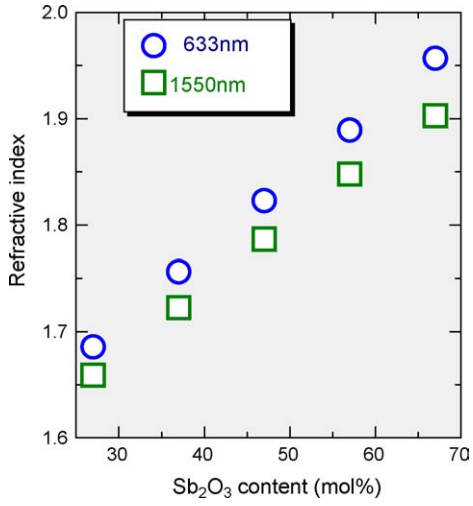

Fig. 1. Compositional dependence of refractive index in $x$$Sb_2O_3$–$(97-x)$ SiO_2–$3Al_2O_3$–$0.5Er_2O_3$ glasses.

was 1.66–1.90, which increased with increasing Sb_2O_3 content.

Fig. 2 shows emission spectra of the $^4I_{13/2} \rightarrow {}^4I_{15/2}$ of Er^{3+} ions in the $x$$Sb_2O_3$–$3Al_2O_3$–$(97-x)SiO_2$ glasses, in the $75TeO_2$–$20ZnO$–$5Na_2O$–$0.5Er_2O_3$ and in the $95SiO_2$–$5GeO_2$–$0.5Er_2O_3$ as a reference. The spectrum of the silica shows the narrowest bandwidth of about 30 nm and that of the tellurite was 60 nm width. It is seen that the Sb_2O_3-based glasses show spectra comparable or broader than that of the tellurite.

Fig. 3 shows the compositional dependence of fluorescence lifetime, τ_f of the $^4I_{13/2}$ level in the $x$$Sb_2O_3$–$3Al_2O_3$–$(97-x)SiO_2$–$0.5Er_2O_3$ glasses. In the range of Sb_2O_3 content $x=37$–67, the fluorescence lifetimes of the $^4I_{13/2}$ level were almost unchanged, and

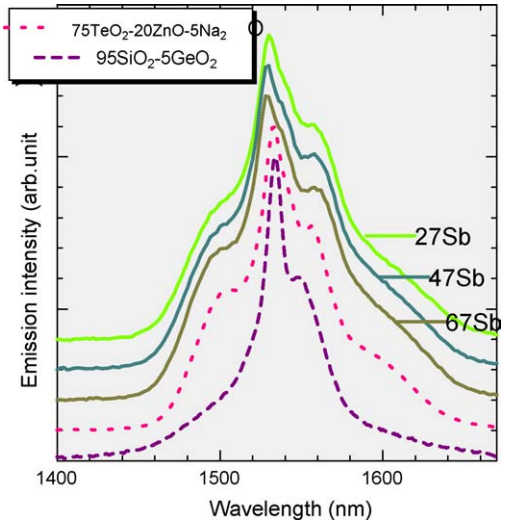

Fig. 2. Fluorescence spectra of $x$$Sb_2O_3$–$(97-x)SiO_2$–$3Al_2O_3$–$0.5Er_2O_3$ glasses.

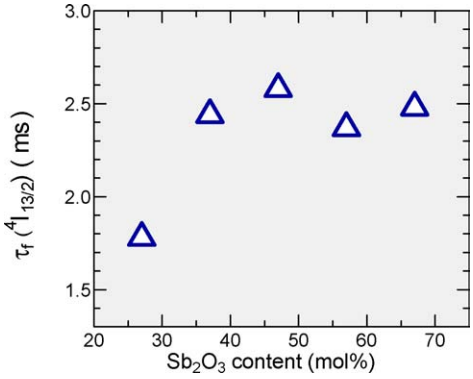

Fig. 3. Compositional dependence of lifetime of Er^{3+}: $^4I_{13/2}$ level in glasses.

about 2.5 ms, whereas in the Sb_2O_3 content $x = 27$, the lifetime was dramatically decreased.

The excitation spectrum associated with Eu^{3+}: $^5D_2 \leftarrow {}^7F_0$ transition for the $x Sb_2O_3$–$3Al_2O_3$–$(97-x)SiO_2$–$0.5Er_2O_3$ glasses are shown in Fig. 4. The intense band due to the pure electronic transition (PET) Eu^{3+}: $^5D_2 \leftarrow {}^7F_0$ transition is located around 464 nm, while the phonon sideband (PSB) coupled to the rare-earth ions is observed in the higher energy range [8]. The position and shape of the phonon sideband were almost unchanged with Sb_2O_3 content.

3.2. Local structure of rare-earth Ions in Sb_2O_3-based glass

Fig. 5 shows the calculated spontaneous emission probability, A, of the $^4I_{13/2} \rightarrow {}^4I_{15/2}$ in the $x Sb_2O_3$–$3Al_2O_3$–$(97-x)SiO_2$–$0.5Er_2O_3$ glasses. The A also increased with increasing x, being nearly 200 s^{-1}. The large A is mainly due

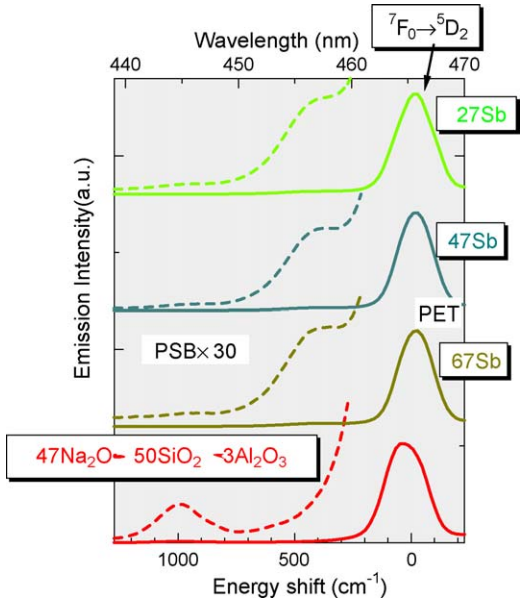

Fig. 4. Excitation spectra of Eu^{3+}-doped glasses. Phonon sideband can be seen in the higher energy side of $^5D_2 \leftarrow {}^7F_0$ transition.

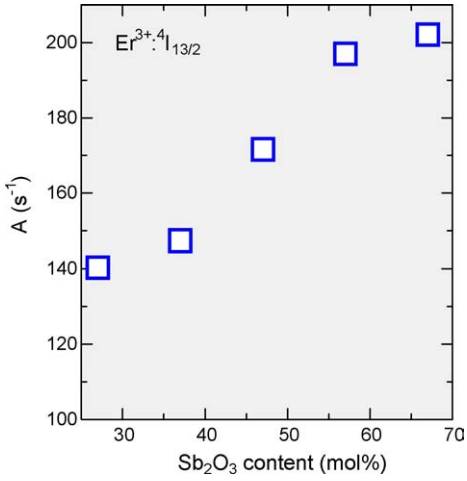

Fig. 5. Compositional dependence of spontaneous emission rate of Er^{3+}: $^4I_{13/2}$ level in glasses.

to large n of the host glasses, which are composed of large amount of Sb^{3+} ion, a p-block element of $5s^2$ electrons having large polarizability [11].

With the measured lifetime and $A_{JJ'}$ from Eq. (1), radiative quantum efficiency, η, was calculated by

$$\eta = \frac{\sum A}{\sum A + \sum W_{NR}} = \tau_f \sum A \quad (2)$$

and plotted in Fig. 6. Reflecting the compositional variations of $A_{JJ'}$, the η increased with increasing Sb_2O_3 content, x. The η values are relatively small compared with those of EDFAs ever reported, but still much larger than that of Pr-doped fiber amplifiers (4%), which perform large gain at 1.3 μm [12]. These low values obtained may be due to lower estimation of real local refractive index, i.e., deviation from measured average index. This can be related with no compositional dependence of the local phonon energy obtained from phonon sideband spectra.

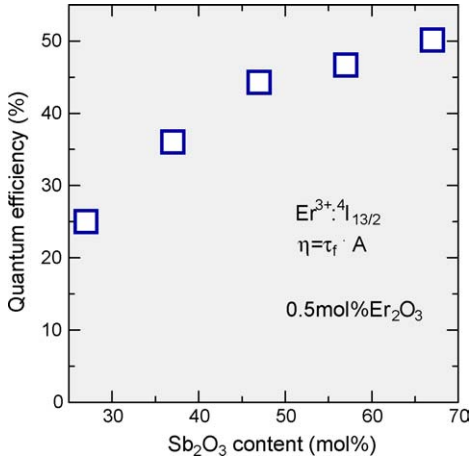

Fig. 6. Compositional dependence of quantum efficiency of Er^{3+}: $^4I_{13/2}$ level in glasses.

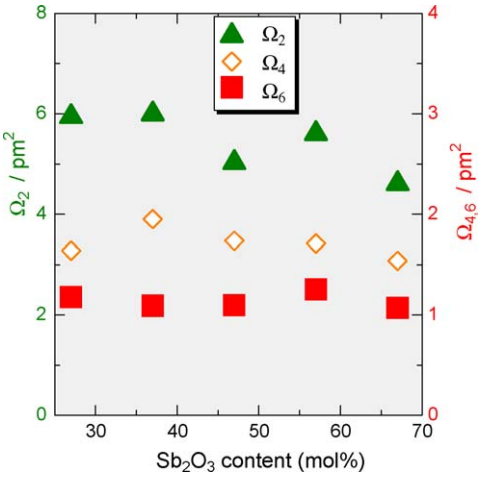

Fig. 7. Composiotional dependence of Judd–Ofelt Ω_t parameters of Er^{3+} ions.

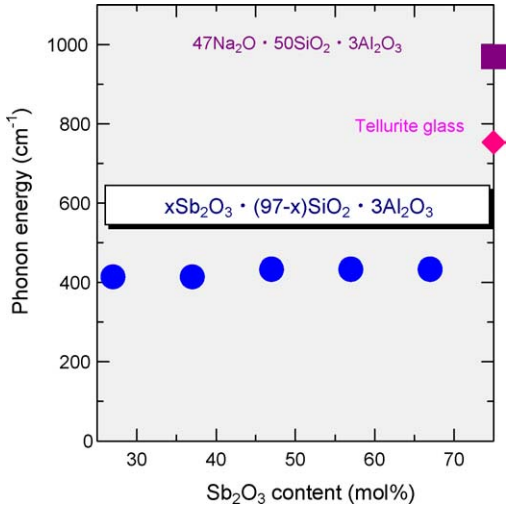

Fig. 8. Compositional dependence of phonon energy from PSB spectra.

Fig. 7 shows the Judd–Ofelt parameters obtained by using the five electric-dipole transition bands. It is seen that the Ω_6 values were almost unchanged with Sb_2O_3 content. These results suggest that the Er^{3+} ions are surrounded selectively by Sb_2O_3-rich phase. Generally, the A of the $^4I_{13/2}$–$^4I_{15/2}$ band is related with the line strengths, S of electric-dipole (ED) and magnetic-dipole (MD) components by [13],

$$A_{JJ'} = \frac{64\pi^4 e^2}{3h(2J'+1)\lambda^3}\left\{\frac{n(n^2+2)^2}{9}\times S^{\mathrm{ED}}_{JJ'} + n^3 \times S^{\mathrm{MD}}_{JJ'}\right\} \quad (3)$$

where e is the elementary charge and h is the Planck constant. The MD transition is independent of the ligand field and contributes to a sharp central peak of spectra around 1.53 μm. Because the S^{MD} is characteristic only to the transition determined by the quantum numbers [14], one of the important factors affecting the compositional variations of the emission properties is the ED transition. The S^{ED} of the $^4I_{13/2}$–$^4I_{15/2}$ is obtained with the Judd–Ofelt parameters and reduced matrix elements by [15,16],

$$S^{\mathrm{ED}}[^4I_{13/2};{}^4I_{15/2}] = 0.019\Omega_2 + 0.118\Omega_4 + 1.462\Omega_6 \quad (4)$$

According to Eq. (4), the Ω_6 plays the most dominant role on the cross-section of the 1.5 μm band among three Ω_t's. Thus, in order to increase the bandwidth of spectra, which is varied with local structure, the increase of the Ω_6 would be effective, because the ED contributes not only to increase the band intensity of the 1.5 μm band but also to broaden the bandwidth [16]. The large Ω_6 value and refractive index may contribute to broad bandwidth in these glasses.

Fig. 8 shows the compositional dependence of the phonon energy, $\hbar\omega$, obtained from the wavelength of the phonon sideband and that of the pure electronic transition. The phonon energy was found to be about 400 cm^{-1} in all the compositions up to 70 mol% SiO_2 content. Usually, in most silicate glasses, the Si–O stretching mode is coupled to the rare-earth ions even in low SiO_2 composition. The present results are in contrast to the above facts and thus suggest that the Er^{3+} ions are surrounded selectively by Sb_2O_3-rich phase and are not affected by Si–O vibration with about 1000 cm^{-1} energy.

3.3. Origin of "non-silicate" environment

Fig. 9 shows the TEM image and a structural model of the glass, where the nano-scale phase separation can be observed [17]. The dark region can be Sb_2O_3-rich phase and the other can be SiO_2-rich phase. Since the solubility of rare-earth ions in a pure silica or silica-rich glass is very low [18], Er^{3+} ions can be condensed in the Sb_2O_3-rich phase, as indicated in the spectroscopic results mentioned above. The concentration dependence of lifetime of Er^{3+}: $^4I_{13/2}$ shows more rapid decrease in a Sb_2O_3 poor composition, indicating that Er^{3+} ions are more condensed. The tendency is moderate in glasses with Sb_2O_3-rich compositions.

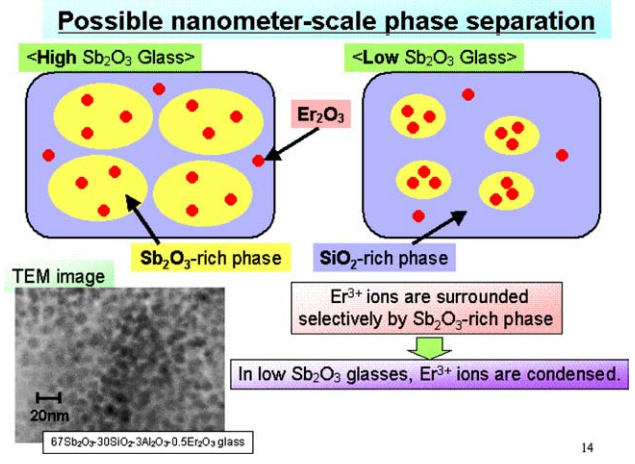

Fig. 9. TEM image of the glass and structural model of nano-scale phase separation.

4. Conclusions

The Sb_2O_3–silicate glasses showed broad emission spectra of 1.5 μm with a large cross-section of Er^{3+} ions. Even the glasses with low Sb_2O_3 content showed broader emission band than the tellurite glass. It is suggested that the nanoscale phase separation exist in these glasses and the Er ions are selectively condensed in the Sb_2O_3-rich phase.

Acknowledgment

This work was supported by Grants-in-Aid for Scientific Research from MEXT.

References

[1] S. Tanabe, C.R. Chim. 5 (2002) 815–824.
[2] S. Tanabe, Properties of Tm-doped tellurite glasses for 1.4 μm amplifier, in: Rare-Earth-Doped Materials and Devices V, SPIE, vol. 4282, 2001, pp. 85–92.
[3] J.S. Wang, E.M. Vogel, E. Snitzer, Opt. Mater. 3 (1994) 187.
[4] A. Mori, Y. Ohishi, S. Sudo, Electron. Lett. 33 (10) (1997) 863–864.
[5] S. Tanabe, N. Sugimoto, S. Ito, T. Hanada, J. Lumin. 87 (2000) 670–672.
[6] J. Minelly, A. Ellison, Opt. Fiber Tech. 8 (2002) 123–138.
[7] S. Tanabe, T. Hanada, J. Non-Cryst. Solids 196 (1996) 101–105.
[8] S. Tanabe, T. Ohyagi, T. Todoroki, T. Hanada, N. Soga, J. Appl. Phys. 73 (12) (1993) 8451–8454.
[9] S. Tanabe, K. Takahara, M. Takahashi, Y. Kawamoto, J. Opt. Soc. Am. B 12 (5) (1995) 786–793.
[10] S. Tanabe, S. Todoroki, K. Hirao, N. Soga, J. Non-Cryst. Solids 122 (1990) 59–65.
[11] W.H. Dumbaugh, Phys. Chem. Glasses 27 (1986) 119.
[12] Y. Ohishi, J. Temmyo, Bull. Ceram. Soc. Jpn. 28 (1993) 110–14.
[13] R.D. Peacock, in: J.D. Dunitz, et al. (Eds.), Structure and Bonding, vol. 22, Springer-Verlag, Berlin, 1975, pp. 83–122.
[14] W.T. Carnall, P.R. Fields, K. Rajnak, J. Chem. Phys. 49 (10) (1968) 4424–4442.
[15] M.J. Weber, Phys. Rev. 157 (2) (1967) 262–272.
[16] S. Tanabe, J. Non-Cryst. Solids 259 (1999) 1–9.
[17] M. Onishi, S. Tanabe, K. Hirao, Technical Digest of Optical Amplifiers and Their Applications 2003, WC3, pp. 248–250 (Otaru, July).
[18] K. Arai, H. Namikawa, K. Kumata, T. Honda, H. Ishii, T. Handa, J. Appl. Phys. 59 (10) (1986) 3430–3436.